Tyng et al. Applied Cancer Research (2018) 38:9
https://doi.org/10.1186/s41241-018-0060-1

Applied Cancer Research

RESEARCH ARTICLE Open Access

# Correlation of the ADC values assessed by diffusion-weighted MRI and $^{18}$F–FDG PET/CT SUV in patients with lung cancer

Chiang Jeng Tyng[1], Marcos Duarte Guimarães[1], Almir Galvão Vieira Bitencourt[1*], Luiz Carlos Mattos dos Santos[1], Paula Nicole Vieira Pinto Barbosa[1], Charles Edouard Zurstrassen[1], Eduardo Nóbrega Pereira[1], Jefferson Luiz Gross[2] and Rubens Chojniak[1]

## Abstract

**Background:** Diffusion-weighted magnetic resonance imaging (DW-MRI) provides information on the cellularity and movement of water molecules in tissues and 18F–fluorodeoxyglucose (18F–FDG) positron emission tomography/computed tomography (18F–FDG PET/CT) assesses cellular glucose metabolism, however both variables are related to tumour aggressiveness. The aim of this study is to investigate the potential correlation of the apparent diffusion coefficient (ADC) assessed by diffusion-weighted MRI (DWI) and glucose metabolism determined by the standardized uptake value (SUV) calculated from $^{18}$F–FDG PET/CT data in non-small cell lung cancer (NSCLC) with the occurrence of metastasis to the lymph nodes.

**Methods:** $^{18}$F–FDG PET/CT and DWI (TR/TE, 1800/93 ms; b-values, 0 and 600 s/mm$^2$) were performed in 37 consecutive patients with histologically verified NSCLC. $SUV_{max}$ was calculated based on the PET-CT data. The minimum ADC ($ADC_{min}$) was determined by placing a region-of-interest (ROI) covering the entire tumou. Results of $^{18}$F–FDG PET/CT and DWI were compared on a per-patient basis. Pearson's correlation coefficient was used for statistical analysis.

**Results:** Correlation analysis of the $ADC_{min}$ and $SUV_{max}$ revealed that the inverse correlation was good for all the masses ($p < 0.001$) and the lymph nodes ($p < 0.001$) for each histological subtype, for both adenocarcinomas ($p < 0.001$) lymph nodes ($p = 0.005$) and squamous cell carcinomas ($p < 0.001$). No significant correlation was found in the comparison of the $ADC_{min}$ and $SUV_{max}$ of the lymph nodes for squamous cell carcinomas ($p = 0.066$).

**Conclusions:** This study verified the relationship between the $SUV_{max}$ and the $ADC_{min}$ in NSCLC. The significant inverse correlation of these two quantitative imaging approaches highlights the association between metabolic activity and tumour cellularity. Therefore, DWI with ADC measurement might represent a new biomarker in NSCLC.

**Keywords:** Magnetic resonance imaging, Positron-emission tomography, lung neoplasms

## Background

Lung cancer is the leading cause of cancer deaths globally, and accounts for more deaths annually than breast, prostate and colon cancer combined [1]. Tumors that are not diagnosed in the early (pre-invasive) stage may infiltrate adjacent structures and metastasize to regional lymph nodes or distant organs. Metastatic events have an important effect on disease progression and mortality.

Diagnostic imaging methods such as computed tomography (CT), positron emission tomography/computed tomography (PET/CT), magnetic resonance imaging (MRI) and bone scintigraphy are routinely performed for detection and staging of primary lung cancer. In the last decade, 18F–fluorodeoxyglucose (18F–FDG) whole body PET/CT examination has been established as the multiparametric imaging method of choice in patients with lung cancer because it allows the investigator to obtain information on tumour morphology, extent and glucose metabolism by calculating the standard uptake value (SUV) [2, 3]. The higher the SUV value, the higher the

* Correspondence: almirgvb@yahoo.com.br
[1]Imaging Department – A.C. Camargo Cancer Center, Rua Prof. Antônio Prudente, 211, São Paulo, SP CEP: 01509-010, Brazil
Full list of author information is available at the end of the article

glycolytic metabolism in the lesion. A strong correlation was observed between the SUV and the clinical course of lung cancer and a poorer therapeutic response if there was no early decrease in SUV after initiation of treatment [4]. Therefore, the SUV is currently considered as an important prognostic factor for lung cancer [5].

High resolution MRI scans can be performed to reliably detect malignant lung lesions and to obtain morphological information about the tumour in the absence of ionizing radiation, an advantage over the CT and PET-CT [6]. Recently, diffusion-weighted magnetic resonance imaging (DW-MRI) has been successfully applied to evaluation of the thorax and has demonstrated great potential in the detection and interpretation of solid lung lesions [7]. In malignant tumours, increased cell density restricts the diffusion of water molecules into the interstitial space, resulting in lower apparent diffusion coefficient (ADC) values. Therefore, diffusion in lung cancer reveals information on cellularity and tumour aggressiveness [7, 8].

The individualization of patient care to optimize therapeutic responses and minimize toxicities is one of the main goals of modern oncology and requires the development of accurate and quantifiable noninvasive markers for prognostic evaluation and early response to treatment [9]. Although DW-MRI provides information on the cellularity and movement of water molecules in tissues and 18F–FDG PET/CT assesses cellular glucose metabolism, both variables are related to tumour aggressiveness. Thus, the aim of this study was to assess the correlation between ADC values in DW-MRI and SUV values in 18F–FDG PET/CT in patients with non-small cell lung cancer (NSCLC).

## Methods

This prospective, unicentric, non-randomized study was conducted based on the collection of data from all adult patients with histologically confirmed NSCLC who were referred for 18F–FDG PET/CT examination for staging at a cancer centre from January 2014 to June 2015. The study was approved by the institution's Research Ethics Committee prior to the beginning of data collection. Patients with histological diagnosis of NSCLC (histological subtypes: squamous cell carcinoma and adenocarcinoma), with pre-therapeutic staging according to the routine of the institution, considering all stages and absence of previous antineoplastic treatment, were included in the study. Patients with contraindications for MRI or who did not sign the consent form were excluded.

Routinely performed imaging tests for NSCLC patients at the institution include 18F–FDG PET/CT and brain MRI. For the present study, when the patient was subjected to brain MRI, thoracic diffusion-weighted sequences were added for evaluation of the primary lung lesion and metastatic mediastinal lymph nodes. Information such as histological type and degree of differentiation were evaluated from the histopathological analysis performed after the initial diagnostic biopsy or after surgical resection of the lesion, when indicated.

The 18F–FDG PET/CT examinations were performed according to the protocol established at the institution using GEMINI Philips PET/CT equipment. All patients underwent 6 h of fasting and received a standard intravenous injection dose of 560 MBq of 18F–FDG. The capillary glycemia was verified before venous injection of 18F–FDG and should have a value lower than 200 mg/dl. The images were obtained 1 h after the injection of the radiopharmaceutical using a high-sensitivity, two-dimensional mode with axial cuts of 10 mm and a matrix of 256 × 256. Later, the images were reconstructed using a 128 × 128 matrix and a filter of 7.0 mm. Eventually, fine adjustments guided by the tomographic examination were necessary to correct the PET images in the analysis of the SUV. PET and CT images were analysed together for anatomical and functional correlations and were sent to a workstation where reconstructions were performed using specific algorithms. All data of interest visually observed on the PET scan were compared with the CT scan to make sure that the non-tumour regions were excluded from the analysis. The 18F–FDG PET/CT images were independently evaluated by two experienced nuclear physicians who performed qualitative (visual) and semiquantitative analyses by calculating the 18F–FDG maximum SUV ($SUV_{max}$) values in the lesions. The $SUV_{max}$ was obtained by selecting the most representative volumetric region of interest (ROI) within the tumour lesion.

Chest MRI scans were performed using a 1.5 T device (Signa Excite HD, GE Healthcare, Milwaukee, WI, USA) with a body coil and a maximum gradient power of 33 mT/m and a pulse rate of 160 mT/m/s. The diffusion sequence was obtained by ultra-fast echoplanar images (IEP) in the axial plane, centred on the lesions and using the following parameters: b values = 0 and 600 s/mm$^2$; TR/TE = 1800/93.8 ms; matrix = 160 × 192; FOV = 360 mm; NEX = 16; number of cuts = 10; cutting thickness = 5 mm; range = 0 mm; approximate total acquisition time = 30 min. The images were transferred to a workstation (Advantage Windows version 4.2_07, GE Healthcare, Milwaukee, WI, USA) and the broadcast sequence was post processed with commercial software (Functool, GE Healthcare, Milwaukee, WI, USA) for the purpose of obtaining ADC maps (blacK/ white and coloured, the latter with Put-thallium pattern, ranging from black colour representing restricted diffusion to red colour which represents no restriction).

The signal intensity and ADC value of NSCLC-related lesions were analysed, through the selection of ROI according to the image interpretation performed by two radiologists

with extensive experience (more than 10 years) in oncology and thoracic Imaging, taking into account the localization, size of lesions and the viable tumour. The ADC calculation for the lesion was performed by linear regression analysis of the natural log of the signal intensity versus the gradient factor according to the following equation: ADC = – (In [Sh / Si]) / (bh - bi). Sh and Si are the signal intensities in the ROI obtained by the difference between two gradient factors (bh and bi). In the present study, the maximum gradient factor (bh) was 600 s/mm$^2$ and the minimum gradient factor (bi) was 0 s/mm$^2$. The ROI most representative of the lesion was always chosen, excluding areas of necrosis, calcifications, gaseous material or areas that suffer interference of some type of partial volume adjacent to the lesion.

Histological data were obtained from the reports of the Department of Pathology. The histological type was defined according to World Health Organization criteria. Tumours were divided into two groups based on the degree of differentiation: poorly differentiated and moderately/well differentiated.

The collected information formed a database developed in the program Excel® for Windows and the statistical analysis was carried out using SPSS® 16.0 software. The categorical variables were presented in absolute and relative frequencies. Continuous variables were described with measures of central tendency (mean and median) and dispersion (standard deviation, minimum and maximum). The statistical significance of the mean differences between the quantitative variables was verified by means of the unpaired Student's t-test or ANOVA, when indicated. The normality of the variables was tested by the Shapiro-Wilk test. For correlation between the values of $SUV_{max}$ and $ADC^{min}$, the Pearson correlation coefficient (r) was used. All analyses were performed using a significance level of 5%, and therefore, the results considered as statistically significant were those whose $p$ value was less than 0.05, always considering two-tailed alternative hypotheses.

## Results

### Characteristics of patients

We evaluated 37 patients, 21 males (56%) and 16 females (44%). The patient ages ranged from 32 to 88 years, with a mean of 64.1 years and median of 63.0 years (standard deviation: 11.4 years).

The most common histological type was adenocarcinoma ($n$ = 21, 56.7%), being considered poorly differentiated in 10 cases (47.6%) and moderately/well differentiated in 11 cases (52.4%). The second most common histological type was squamous cell carcinoma ($n$ = 16 cases, 43.2%). It was considered to be poorly differentiated in 10 cases (62.5%) and moderately/well differentiated in six cases (37.5%).

No significant differences between the different histological types were found in the values of $ADC_{min}$ or $SUV_{max}$ in the primary tumour ($p$ = 0.484 for $ADC_{min}$; $p$ = 0.165 for max SUV). Poorly differentiated tumours presented lower values of $ADC_{min}$ (1.34 ± 0.52 vs. 1.78 ± 0.79, $p$ = 0.060) and higher values of $SUV_{max}$ (9.32 ± 4.52 vs. 6.25 ± 2.81, $p$ = 0.027), when compared to moderate/well differentiated tumours.

### Correlation between $ADC_{min}$ and $SUV_{max}$

Table 1 shows the values of $SUV_{min}$ and $ADC_{max}$ of all lung masses and lymph nodes. Figure 1 shows a negative correlation for both mass and lymph nodes (high values of $ADC_{min}$ are associated with low values of $SUV_{max}$). The Pearson correlation coefficient for mass ($r$ = – 0.806) was stronger than for lymph nodes ($r$ = – 0.592), but both were highly significant ($p$ < 0.001).

Table 2 shows the $SUV_{min}$ and $ADC_{min}$ values of the lung masses and lymph nodes, only in the group of patients with adenocarcinoma. Figure 2 shows a negative correlation for both mass and lymph nodes (high values of $ADC_{min}$ are associated with low values of $SUV_{max}$). The Pearson correlation coefficient for mass ($r$ = – 0.739, $p$ < 0.001) was stronger than for lymph nodes ($r$ = – 0.660, $p$ = 0.005).

Table 3 shows values of the $SUV_{max}$ and $ADC_{min}$ of the lung masses and lymph nodes, only of the group of patients with epidermoid carcinoma. Figure 3 shows a negative correlation for both the mass ($r$ = – 0.900; $p$-value < 0.001) and lymph nodes ($r$ = – 0.486; $p$-value = 0.066); however, the correlation coefficient for the lymph nodes was not statistically significant.

## Discussion

The present study demonstrated the existence of a significant inverse correlation between $ADC_{min}$ and $SUV_{max}$ in primary lung tumours, regardless of histological subtype. Our results are in agreement with the study of Regier et al. [10], who verified the significant inverse correlation between these two quantitative variables ($ADC_{min}$ x $SUV_{max}$) in 41 patients evaluated with NSCLC [10]). These results demonstrate that there is a direct relationship between the mobility of water molecules in the tissue evaluated by DW-MRI and glycolytic metabolism evaluated by PET/CT, possibly related to tumour aggressiveness.

**Table 1** Values of $ADC_{min}$ and $SUV_{max}$ in all patients with lung cancer

| Variable | N | Average | S.D. | Minimum | Medium | Maximum |
|---|---|---|---|---|---|---|
| Mass ADC | 37 | 1,60 | 0,71 | 0,59 | 1,40 | 3,80 |
| LN ADC | 31 | 3,01 | 1,55 | 0,72 | 3,20 | 6,86 |
| Mass SUV | 37 | 7,71 | 4,21 | 1,90 | 7,00 | 19,10 |
| LN SUV | 31 | 6,26 | 3,98 | 1,80 | 4,70 | 17,30 |

*S.D.* standard deviation, *ADC* apparent diffusion coefficient, *LN* lymph node, *SUV* standard uptake value

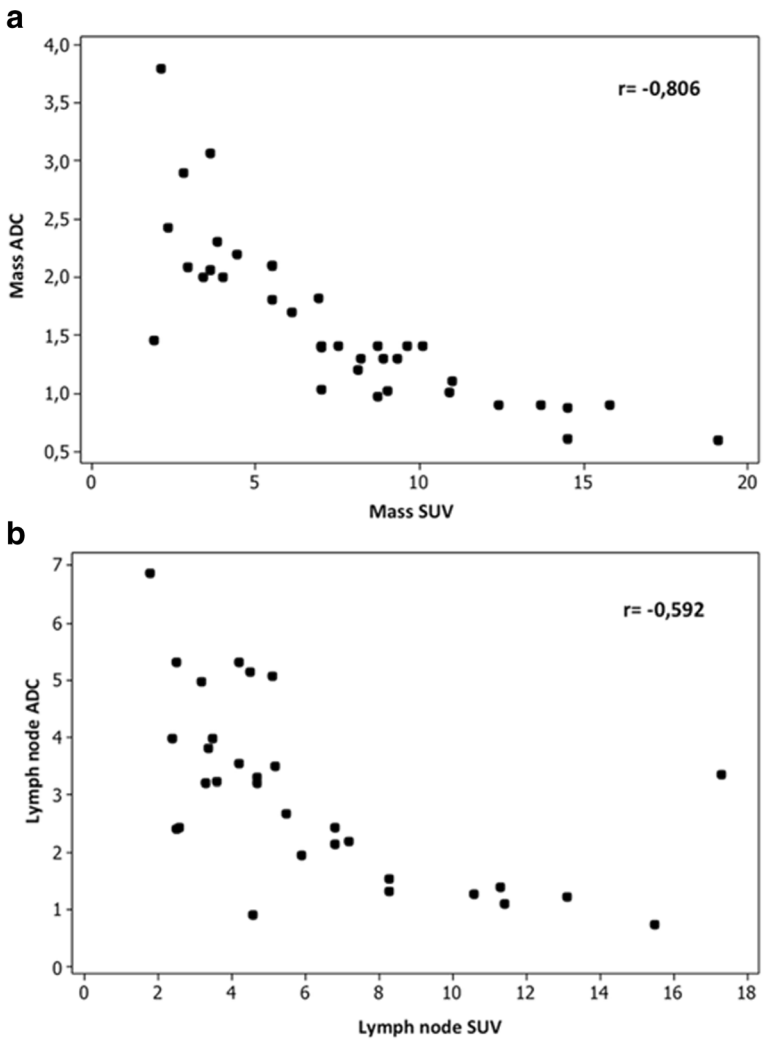


**Fig. 1** Scatter plots of the $ADC_{min}$ against $SUV_{max}$ for masses a and lymph nodes **b** in all patients with lung cancer

In PET/CT the detected activity of 18F–FDG represents an analogy of tumour glucose metabolism. High uptake of FDG reflects an increase in glycolysis and metabolic activity of malignant tumours and allows this technique to obtain information on pathophysiological activity and tumour proliferation by determining the SUV. In DW-MRI, a reduction in ADC levels has been shown to be indicative of various malignant diseases [11], tumour characteristics, the manifestation of lymph node metastases [12] and response to antitumour treatment [13]. Therefore, both approaches, the SUV revealing the tumor metabolism on one hand and the ADC demonstrating diffusion restriction due to a change in the microstructural tumour environment on the other hand, are in direct relation to tumour aggressiveness.

**Table 2** Values of $ADC_{min}$ and $SUV_{max}$ only in the group of patients with adenocarcinoma

| Variable | N | Average | S.D. | Minimum | Medium | Maximum |
|---|---|---|---|---|---|---|
| Mass ADC | 21 | 1,61 | 0,69 | 0,90 | 1,40 | 3,80 |
| LN ADC | 16 | 3,73 | 1,48 | 1,52 | 3,52 | 6,86 |
| Mass SUV | 21 | 6,99 | 3,52 | 1,90 | 7,00 | 15,80 |
| LN SUV | 16 | 4,53 | 1,85 | 1,80 | 4,35 | 8,30 |

*S.D.* standard deviation, *ADC* apparent diffusion coefficient, *LN* lymph node, *SUV* standard uptake value

These results confirm the assumption that DW-MRI may have a role in the imaging evaluation of NSCLC; however, its full diagnostic capacity has not yet been explored. Until now, only a few studies have investigated the relationship between DW-MRI and 18F–FDG PET/CT. Palumbo et al. [14] investigated 15 patients with various types of brain metastases and observed the inverse correlation between low ADC values and 18F–FDG PET/CT hypermetabolism. In 9 of these patients, the primary malignant disease was NSCLC [14].

The observation of this correlation raises a hypothesis that the quantitative DW-MRI may have a role as a

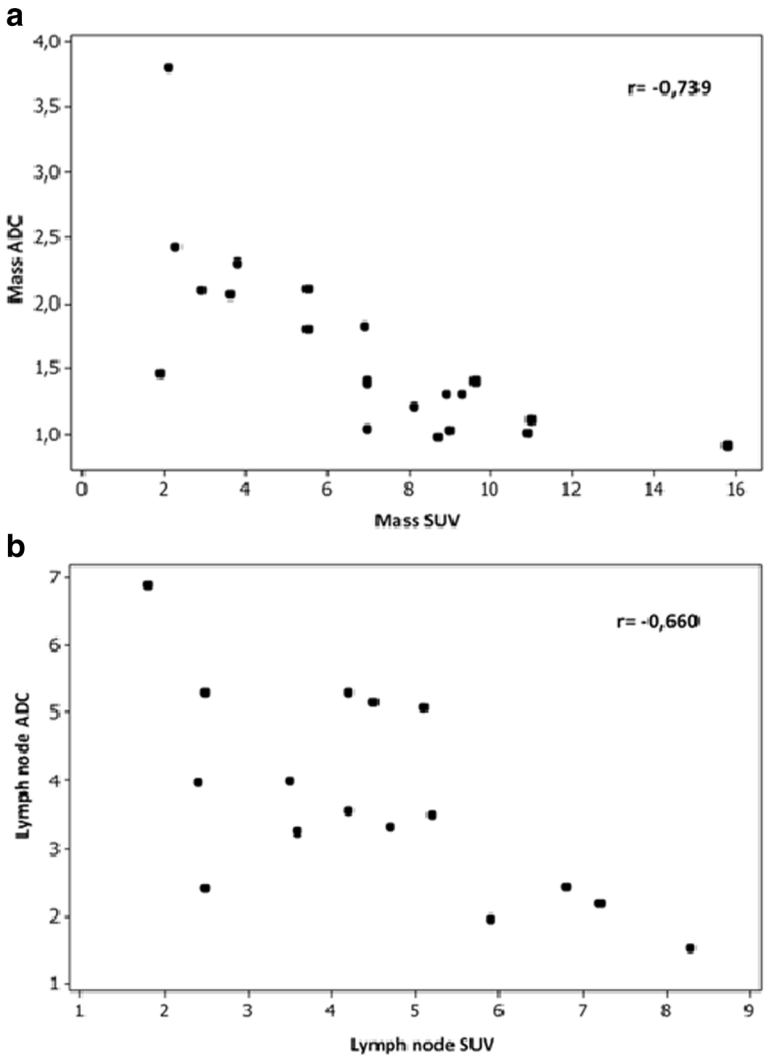


**Fig. 2** Scatter plots of the $ADC_{min}$ against $SUV_{max}$ for masses **a** and lymph nodes **b** only in the group of patients with adenocarcinoma

biomarker for prognosis evaluation in NSCLC, similar to 18F–FDG PET/CT. It has been reported that high SUV determined in the primary tumour prior to treatment is associated with a shorter time to progression, higher recurrence rates and lower overall survival rates [15]. Furthermore, it has been demonstrated that if there is no reduction of $SUV_{max}$ early after initiation of anticancer treatment, there will be no substantial response to therapy and limited survival [4]. Thus, the SUV is often recognized as a prognostic biomarker in NSCLC patients [5].

**Table 3** Values of $ADC_{min}$ and $SUV_{max}$ only in the group of patients with epidermoid carcinoma

| Variable | N | Average | S.D. | Minimum | Medium | Maximum |
|---|---|---|---|---|---|---|
| Mass ADC | 16 | 1,58 | 0,75 | 0,59 | 1,41 | 3,07 |
| LN ADC | 15 | 2,24 | 1,26 | 0,72 | 2,14 | 4,97 |
| Mass SUV | 16 | 8,66 | 4,93 | 2,80 | 7,85 | 19,10 |
| LN SUV | 15 | 8,11 | 4,81 | 2,60 | 6,80 | 17,30 |

*S.D.* standard deviation, *ADC* apparent diffusion coefficient, *LN* lymph node, *SUV* standard uptake value

The results of this study may suggest the use of DW-MRI as a tool for evaluating tumour response to chemotherapy. Until now, a reduction in diameter or volume determined in serial CT studies represented the established indicator of tumour response to treatment. The main disadvantage of size measurement is the range of 0–8 weeks required to detect size reduction. As chemotherapy leads to a rupture of the cell membranes and the reduction of cell size and density, the diffusion of the molecules increases rapidly after the beginning of the treatment [13]. Therefore, DW-MRI has the potential to evaluate the treatment response at an earlier stage, as the increase in ADC may precede the reduction of tumour size.

However, while 18F–FDG PET/CT has already been successfully integrated into the daily clinical care of NSCLC patients, more studies will be needed to

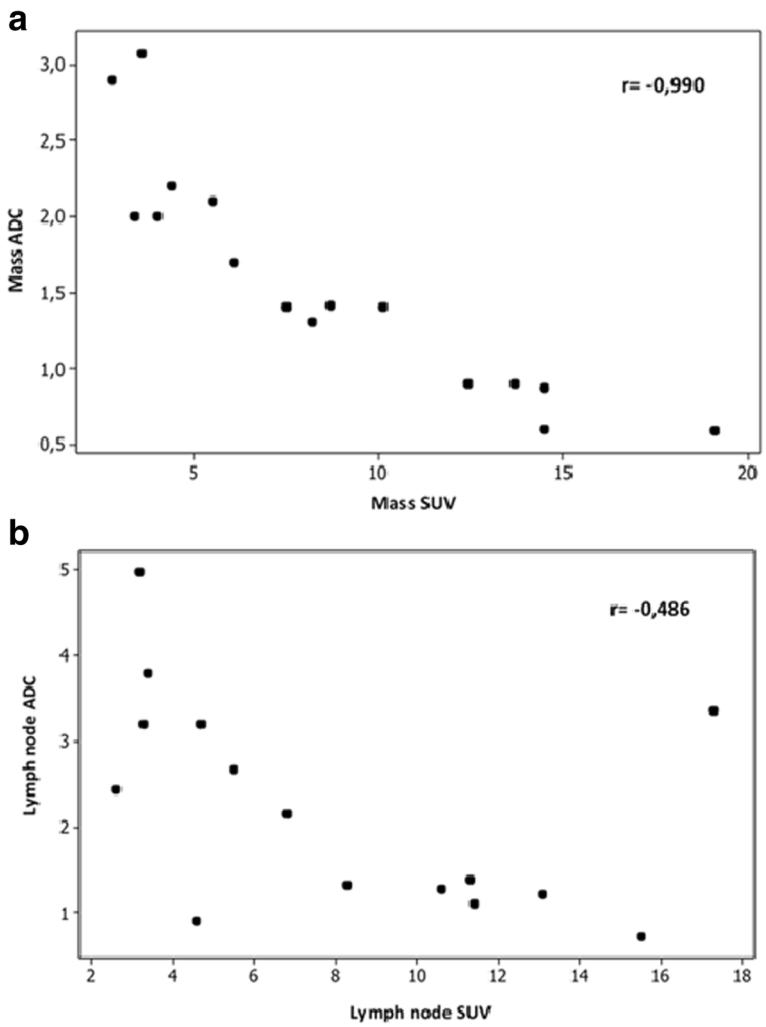


**Fig. 3** Scatter plots of the $ADC_{min}$ against $SUV_{max}$ for masses **a** and lymph nodes **b** only in the group of patients with epidermoid carcinoma

investigate whether the correlation of ADC and SUV can prove to have prognostic significance or predictability in the therapeutic response of DW-MRI in this population. Besides that, there is a higher variability in ADC measurements in different institutions. To obtain ADC value, it's necessary more than 20 parameters in MRI setup, which difficult a protocol standardization in DW sequences, as example: cutting thickness, number of cuts, FOV, temperature, TR/TE, total acquisition time and others.

We observed a statistically significant inverse correlation between SUV and ADC in the compromised adenocarcinoma lymph nodes, but not in the lymph nodes of squamous cell carcinomas. In addition, the presence of 18F–FDG PET/CT showed an evident superiority over CT [16], but false positive results are not uncommon [17]. Usuda et al. [18] observed a greater accuracy of DW-MRI over 18F–FDG PET/CT in the diagnosis of metastatic lymph nodes in patients with NSCLC [18].

We also compared the relationship of ADC and SUV to the degree of tumor differentiation. The poorly differentiated tumours had lower values of $ADC_{min}$ and higher values of $SUV_{max}$, when compared to moderately/well differentiated tumours. However, the difference in $ADC_{min}$ values was not statistically significant. Herneth et al. [19] showed that tissue ADC is determined by cell density and that cell necrosis can improve water diffusibility and increase ADC values before macroscopic changes in histological sections and MR images [19]. Thus, in poorly differentiated tumours with relatively high ADC values, the microstructural changes preceding macroscopic necrosis within the tumour tissue appear to represent a factor influencing the ADC value.

Some limitations of our study should be considered such as the population size. Therefore, our results can be considered only preliminary, utilizing a limited number of well-differentiated NSCLC cases, impairing the statistical analysis of the correlation of ADC and SUV with the histological types and their respective degrees of differentiation.

## Conclusion

The present study demonstrated a significant negative correlation of the SUV values evaluated by 18F–FDG PET/CT and ADC values evaluated by DW-MRI in lung masses and metastatic lymph nodes in patients with NSCLC. Considering the advantages of MRI as an imaging method that does not require ionizing radiation, future studies may better explore the applications of DW-MRI in the prognosis and therapeutic response of lung cancer.

### Abbreviations

18F–FDG: 18F–fluorodeoxyglucose; ADC: Apparent diffusion coefficient; ADCmin: Minimum ADC; CT: Computed tomography; DWI: Diffusion-weighted; DW-MRI: Diffusion-weighted magnetic resonance imaging; MRI: Magnetic resonance imaging; NSCLC: Non-small cell lung cancer; PET/CT: Positron emission tomography/computed tomography; ROI: Region of interest; SUV: Standard uptake value; SUVmax: Maximum SUV

### Acknowledgements

Not applicable.

### Availability of data and materials

The datasets analysed during the current study available from the corresponding author on reasonable request.

### Funding

No funding received.

### Authors' contributions

Chiang Jeng Tyng and Rubens Chojniak designed the research. Chiang Jeng Tyng, Marcos Duarte Guimarães, Almir Galvão Vieira Bitencourt, Luiz Carlos Mattos dos Santos, Paula Nicole Vieira Pinto Barboss, Charles Edouard Zurstrassen, Eduardo Nóbrega Pereira and Jefferson Luiz Gross performed the research and analyzed the data. And all authors wrote/revised the paper. All authors read and approved the final manuscript.

### Ethics approval and consent to participate

This project received approval from the institution's Research Ethics Committee (no1674/12).

### Consent for publication

Not applicable.

### Competing interests

None. All procedures performed in these study were in accordance with the ethical standards of the institutional research committee and with the 1964 Helsinki declaration and its later amendments.

## Publisher's Note



### Author details

[1]Imaging Department – A.C. Camargo Cancer Center, Rua Prof. Antônio Prudente, 211, São Paulo, SP CEP: 01509-010, Brazil. [2]Thoracic Department – A.C. Camargo Cancer Center, Rua Prof. Antônio Prudente, 211, São Paulo, SP CEP: 01509-010, Brazil.

Received: 13 November 2017 Accepted: 22 February 2018
Published online: 02 April 2018

### References

1. McMahon PM, Kong CY, Johnson BE, Weinstein MC, Weeks JC, Kuntz KM, et al. Estimating long-term effectiveness of lung cancer screening in the Mayo CT screening study. Radiology. 2008;248(1):278–87.
2. De Wever W, Stroobants S, Coolen J, Verschakelen JA. Integrated PET/CT in the staging of nonsmall cell lung cancer: technical aspects and clinical integration. Eur Respir J. 2009;33(1):201–12.
3. Kligerman S, Digumarthy S. Staging of non-small cell lung cancer using integrated PET/CT. AJR. 2009;193(5):1203–11.
4. Nahmias C, Hanna WT, Wahl LM, Long MJ, Hubner KF, Townsend DW. Time course of early response to chemotherapy in non-small cell lung cancer patients with 18F-FDG PET/CT. J Nucl Med. 2007;48(5):744–51.
5. Borst GR, Belderbos JSA, Boellaard R, Comans EFI, Jaeger K, Lammertsma AA, et al. Standardised FDG uptake: a prognostic factor for inoperable non-small cell lung cancer. Eur J Cancer. 2005;41(11):1533–41.
6. Regier M, Kandel S, Kaul MG, Hoffmann B, Ittrich H, Bansmann PM, et al. Detection of small pulmonary nodules in high-field MR at 3 T: evaluation of different pulse sequences using porcine lung explants. Eur Radiol. 2007;17(5):1341–51.
7. Matoba M, Tonami H, Kondou T, Yokota H, Higashi K, Toga H, et al. Lung carcinoma: diffusion-weighted mr imaging–preliminary evaluation with apparent diffusion coefficient. Radiology. 2007;243(2):570–7.
8. Takahara T, Imai Y, Yamashita T, Yasuda S, Nasu S, Van Cauteren M. Diffusion weighted whole body imaging with background body signal suppression (DWIBS): technical improvement using free breathing, STIR and high resolution 3D display. Radiat Med. 2004;22(4):275–82.
9. Theilmann RJ, Borders R, Trouard TP, Xia G, Outwater E, Ranger-Moore J, et al. Changes in water mobility measured by diffusion MRI predict response of metastatic breast cancer to chemotherapy. Neoplasia. 2004;6(6):831–7.
10. Regier M, Derlin T, Schwarz D, Laqmani A, Henes FO, Groth M, et al. Diffusion weighted MRI and 18F-FDG PET/CT in non-small cell lung cancer (NSCLC): does the apparent diffusion coefficient (ADC) correlate with tracer uptake (SUV)? Eur J Radiol. 2012;81(10):2913–8.
11. Gourtsoyianni S, Papanikolaou N, Yarmenitis S, Maris T, Karantanas A, Gourtsoyiannis N. Respiratory gated diffusion-weighted imaging of the liver: value of apparent diffusion coefficient measurements in the differentiation between most commonly encountered benign and malignant focal liver lesions. Eur Radiol. 2008;18(3):486–92. https://doi.org/10.1007/s00330-007-0798-4
12. Pauls S, Schmidt SA, Juchems MS, Klass O, Luster M, Reske SN, et al. Diffusion-weighted MR imaging in comparison to integrated [$^{18}$F]-FDG PET/CT for N-staging in patients with lung cancer. Eur J Radiol. 2012;81(1):178–82.
13. Dudeck O, Zeile M, Pink D, Pech M, Tunn PU, Reichardt P, et al. Diffusion-weighted magnetic resonance imaging allows monitoring of anticancer treatment effects in patients with soft-tissue sarcomas. J Magn Reson Imaging. 2008;27(5):1109–13.
14. Palumbo B, Angotti F, Marano GD. Relationship between PET-FDG and MRI apparent diffusion coefficients in brain tumors. J Nucl Med Mol Imaging. 2009;53(1):17–22.
15. Cerfolio RJ, Bryant AS, Ohja B, Bartolucci AA. The maximum standardized uptake values on positron emission tomography of a non-small cell lung cancer predict stage, recurrence, and survival. J Thorac Cardiovasc Surg. 2005;130(1):151–9.
16. Gould MK, Kuschner WG, Rydzak CE, Maclean CC, Demas AN, Shigemitsu H, et al. Test performance of positron emission tomography and computed tomography for mediastinal staging in patients with non-small-cell lung cancer: a meta-analysis. Ann Intern Med. 2003;139(11):879–92.
17. Roberts PF, Follette DM, Von Haag D, Park JA, Valk PE, Pounds TR, et al. Factors associated with false-positive staging of lung cancer by positron emission tomography. Ann Thorar Surg. 2000;70(4):1154. -9-60
18. Usuda K, Zhao XT, Sagawa M, Matoba M, Kuginuki Y, Taniguchi M, et al. Diffusion-weighted imaging is superior to positron emission tomography in the detection and nodal assessment of lung cancers. Ann Thorar Surg. 2011;91(6):1689–95.
19. Herneth AM, Guccione S, Bednarski M. Apparent diffusion coefficient: a quantitative parameter for in vivo tumor characterization. Eur J Radiol. 2003;45(3):208–13.